ChemPubSoc Europe

DOI: 10.1002/chem.201406566

CHEMISTRY
A European Journal
Communication

Photocatalysis

A Si Photocathode Protected and Activated with a Ti and Ni Composite Film for Solar Hydrogen Production

Yi-Hsuan Lai, Hyun S. Park, Jenny Z. Zhang, Peter D. Matthews, Dominic S. Wright, and Erwin Reisner*[a]

Abstract: An efficient, stable and scalable hybrid photoelectrode for visible-light-driven H_2 generation in an aqueous pH 9.2 electrolyte solution is reported. The photocathode consists of a *p*-type Si substrate layered with a Ti and Ni-containing composite film, which acts as both a protection and electrocatalyst layer on the Si substrate. The film is prepared by the simple drop casting of the molecular single-source precursor, $[\{Ti_2(OEt)_9(NiCl)\}_2]$ ($TiNi_{pre}$), onto the p-Si surface at room temperature, followed by cathodic in situ activation to form the catalytically active TiNi film ($TiNi_{cat}$). The p-Si | $TiNi_{cat}$ photocathode exhibits prolonged hydrogen generation with a stable photocurrent of approximately $-5\ mA\,cm^{-2}$ at 0 V vs. RHE in an aqueous pH 9.2 borate solution for several hours, and serves as a benchmark non-noble photocathode for solar H_2 evolution that operates efficiently under neutral–alkaline conditions.

Photoelectrochemical (PEC) water splitting is an attractive strategy to generate the renewable energy carrier hydrogen (H_2).[1] A solar energy conversion efficiency of greater than 20% can theoretically be achieved in a PEC tandem cell with a 1.0 and 1.6 eV band-gap pair of semiconductor electrodes,[2] thereby surpassing the current conversion targets for profitable solar H_2 generation of 15–20%.[3] However, the implementation of PEC water splitting can only be accomplished when such semiconductors are not only efficient, but also stable and scalable.

Crystalline silicon (Si) displays excellent light-harvesting and charge-separation properties, delivering cell efficiencies of up to 25% in photovoltaic cells.[4] Si is also among the most promising and advanced photocathode materials for fuel generation, in particular for PEC water splitting.[5] p-Type Si (p-Si) possesses a small band-gap of 1.1 eV with a suitable conduction band potential of −0.6 V vs. the reversible hydrogen electrode (RHE) for the reduction of aqueous protons. Thus, p-Si shows close-to-ideal solar light-harvesting properties and provides an overpotential (η) of 0.6 V for H_2 generation.

However, several drawbacks must be addressed before p-Si can be used in PEC devices. The surface of Si must be protected under ambient conditions to avoid the rapid formation of silicon oxide at the surface, which may lead to the complete quenching of its photoactivity. Furthermore, an electrocatalyst promoting the hydrogen evolution reaction (HER) must be introduced to its surface to overcome the kinetic barriers associated with proton reduction. Passivation of the semiconductor with a conformal layer of TiO_2 has been shown to protect the electrode from photodecomposition and surface oxidation, and the further introduction of Pt was shown to promote HER in strongly acidic aqueous solution.[5a,b] However, TiO_2 layering requires costly sputtering[5a] and atomic layer deposition (ALD)[5b] techniques, whereas the use of noble metal catalysts is undesirable due to the scarce reserves and high costs. A simple and scalable method for preparing protected Si with an inexpensive and efficient electrocatalyst is therefore required to pave the way for p-Si in PEC devices.

Herein, we report a scalable procedure for protecting and catalytically activating p-Si under ambient conditions using the heterobimetallic single-source precursor $[\{Ti_2(OEt)_9(NiCl)\}_2]$ ($TiNi_{pre}$). Drop casting of the molecular $TiNi_{pre}$ onto p-Si and in situ cathodic activation results in the formation of a protection layer for p-Si and a catalytically active film ($TiNi_{cat}$, Figure 1). This hybrid p-Si | $TiNi_{cat}$ photoelectrode contains only earth-abundant materials and demonstrates good photostabili-

[a] *Y.-H. Lai,[+] Dr. H. S. Park,[+] Dr. J. Z. Zhang, P. D. Matthews, Prof. D. S. Wright, Dr. E. Reisner*
Christian Doppler Laboratory for Sustainable SynGas Chemistry
Department of Chemistry, University of Cambridge
Cambridge CB2 1EW (UK)
E-mail: reisner@ch.cam.ac.uk
Homepage: http://www-reisner.ch.cam.ac.uk/

[+] *These authors contributed equally to this work.*

Supporting information for this article is available on the WWW under http://dx.doi.org/10.1002/chem.201406566.

© 2015 The Authors. Published by Wiley-VCH Verlag GmbH & Co. KGaA. This is an open access article under the terms of the Creative Commons Attribution License, which permits use, distribution and reproduction in any medium, provided the original work is properly cited.

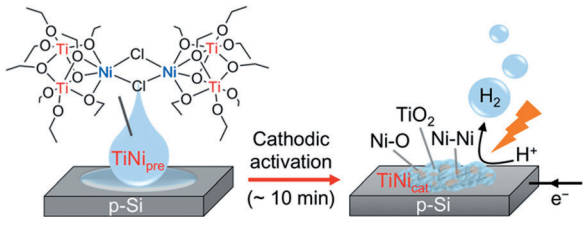

Figure 1. Schematic representation of the preparation of a TiNi-modified p-Si electrode by a dual process: drop casting of $TiNi_{pre}$ followed by in situ cathodic activation to form $TiNi_{cat}$ for protection and catalytic activation of the p-Si photocathode. $TiNi_{pre}$ structure is adopted from X-ray coordinates.

 © 2015 The Authors. Published by Wiley-VCH Verlag GmbH & Co. KGaA, Weinheim

ty for prolonged PEC H_2 generation in near-neutral pH aqueous solution.

The cathodically induced conversion of $TiNi_{pre}$ into the HER electrocatalyst $TiNi_{cat}$ was first investigated on a fluoride-doped tin oxide (FTO)-coated glass substrate by electrochemical methods. A $TiNi_{pre}$ solution (2×20 μL, 5 mM in toluene) was drop casted onto the FTO-coated glass (1 cm^2 exposed surface area) to form the FTO|$TiNi_{pre}$ electrode. The theoretical amount of Ni atoms deposited on the FTO is approximately 0.4 μmol cm^{-2} (see Supporting Information). The FTO|$TiNi_{pre}$ was subsequently used as the working electrode in a two-compartment electrochemical cell containing an aqueous borate (B_i) solution (0.1 M, pH 9.2). The electrochemical experiments were performed at room temperature under N_2 using a conventional three-electrode system, with $Ag/AgCl/KCl_{sat}$ as the reference electrode and Pt foil as the counter electrode.

The FTO|$TiNi_{pre}$ electrode requires chronoamperometric activation for 60 min at an applied potential of −0.49 V vs. RHE (see Supporting Information, Figure S1 a). The current density increased initially and stabilized at −1.45 mA cm^{-2} with the formation of H_2 bubbles (confirmed by gas chromatography). A similar activation process was observed in aqueous phosphate solution (0.1 M P_i, pH 7), but not in Na_2SO_4 (0.1 M, pH 9.2) or $NaNO_3$ solution (0.1 M, pH 9.2; see the Supporting Information, Figure S1). These experiments suggest that the buffer plays an important role in the activation of $TiNi_{cat}$ and its HER activity.

Figure 2 a compares the electrocatalytic activity of different HER catalysts modified on FTO-coated glass in pH 9.2 B_i solution containing KCl (1 M) as the supporting electrolyte. It can be seen in the linear sweep voltammetry (LSV) scans (scan rate of 1 mV s^{-1}) that FTO|$TiNi_{cat}$ exhibits catalytic activity with a small η of approximately 100 mV, catalyzing HER with a respectable current density of −2 mA cm^{-2} at $\eta=420$ mV. Blank FTO and FTO|TiO_2 electrode (prepared by drop casting titanium isopropoxide in toluene on FTO followed by the same cathodic treatment as for FTO|$TiNi_{cat}$; see Supporting Information) exhibited negligible current densities. A metallic Ni HER catalyst (FTO|e-Ni) was electrodeposited on the FTO-coated glass using a B_i buffer solution containing $Ni(NO_3)_2{\cdot}6H_2O$ (0.5 mM; see the Supporting Information and Figure S2).[6] The resulting FTO|e-Ni electrode exhibited lower activity than FTO|$TiNi_{cat}$, generating a current density of −2 mA cm^{-2} at $\eta=$ 490 mV, which is consistent with previously reported results.[6]

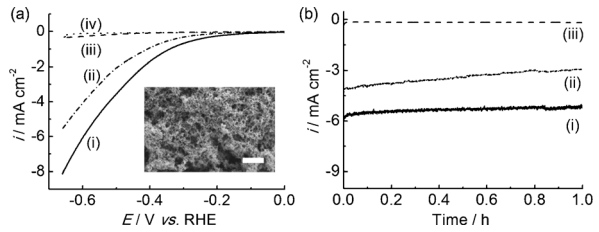

Figure 2. (a) Linear sweep voltammetry (LSV) scans of (i) FTO|$TiNi_{cat}$, (ii) FTO|e-Ni, (iii) FTO|TiO_2, and (iv) FTO in an aqueous buffer solution (0.1 M B_i, 1 M KCl, pH 9.2) at a scan rate of 1 mV s^{-1}. The inset shows the SEM image of FTO|$TiNi_{cat}$ with a scale bar of 2 μm. (b) Chronoamperometric traces at an applied potential of −0.6 V vs. RHE.

The stability of the electrodes was tested by controlled potential electrolysis (CPE) in an aqueous pH 9.2 B_i/KCl electrolyte solution for 1 h at $\eta=0.6$ V (Figure 2 b). FTO|$TiNi_{cat}$ displayed good stability with a steady state current density of approximately −5.5 mA cm^{-2}. FTO|e-Ni showed decreased stability, with a current density of −3.0 mA cm^{-2} remaining after 1 h CPE. Headspace product analysis by gas chromatography confirmed quantitative faradaic efficiency for FTO|$TiNi_{cat}$ (Table 1).

Table 1. Summary of the amount of headspace H_2, the corresponding faradaic efficiency (FE) and TOF of electro- and photocatalytically generated H_2 with $TiNi_{cat}$ in a pH 9.2 B_i (0.1 M)/KCl (1 M) solution.

Electrode	E [V vs. RHE]	H_2 [μmol h^{-1} cm^{-2}]	FE [%]	Ni amount [μmol cm^{-2}][b]	TOF [h^{-1}]
FTO|$TiNi_{cat}$	−0.39	26±4	99±3	0.4	65
FTO|$TiNi_{cat}$	−0.6	96±7	97±2	0.4	240
p-Si|$TiNi_{cat}$[a]	0	74±4	100±5	1.2	>62[c]

[a] Photocatalytic H_2 generation under simulated solar light irradiation (AM 1.5G). [b] The amount of Ni was estimated from the total amount of TiNi drop casted on the electrode (see Supporting Information). [c] The TOF of p-Si|$TiNi_{cat}$ is likely underestimated because significant amounts of TiNi solution leaked during the deposition.

FTO|$TiNi_{cat}$ evolved approximately 26 and 96 μmol h^{-1} cm^{-2} of H_2 at $\eta=0.39$ and $\eta=0.6$ V, respectively. A turnover frequency (TOF; defined as mol H_2 per mol Ni estimated based on all Ni deposited on FTO) of approximately 65 h^{-1} is reached at $\eta=$ 0.39 V (see the Supporting Information), which is comparable with the reported TOF of the non-noble cobalt-based HER catalyst prepared by electrodeposition of a cobalt salt in P_i buffer (80 h^{-1} at $\eta=0.39$ V vs. RHE).[7]

Scanning electron microscopy (SEM) showed a TiNi film thickness of approximately 3 to 4 μm and an unchanged surface morphology of agglomerated particles before and after catalysis (Figure 2 and Figure S3 in the Supporting Information).[8] X-ray diffraction (XRD) studies confirmed an amorphous structure of $TiNi_{pre}$[8] and $TiNi_{cat}$ films (Figure S4). Both $TiNi_{pre}$ and $TiNi_{cat}$ films have no absorption in the visible light regions (Figure S5). X-ray photoelectron spectroscopy (XPS) confirmed that $TiNi_{cat}$ is composed of TiO_2 and Ni with a small amount of boron from B_i (Figure S6). Cl is only observable on the surface of $TiNi_{pre}$ and is absent from the surface after the activation process (Figures S6 and S7). In the Ni 2p region, two broad sets of signals at 855.7 eV ($2p_{3/2}$) and 873.3 eV ($2p_{1/2}$) core levels are present in $TiNi_{cat}$, which can be assigned to $Ni(OH)_2$/NiO_x.[9] No metallic feature of Ni is visible on the surface of FTO|$TiNi_{cat}$, but this can be attributed to any surface metallic Ni being unstable in air, thus becoming oxidized during handling before the XPS measurement. However, a slightly lower binding energy in Ni 2p region is observed for FTO|$TiNi_{cat}$ compared to FTO|$TiNi_{pre}$ (Figure S8), indicating that the composition of the film is likely changed after cathodic activation.

X-ray absorption spectroscopy (XAS) was performed to gain further insights into the average speciation, oxidation state, and local environments of the Ni and Ti atoms throughout the bulk of the amorphous TiNi material. Figure 3 a presents the X-

 © 2015 The Authors. Published by Wiley-VCH Verlag GmbH & Co. KGaA, Weinheim

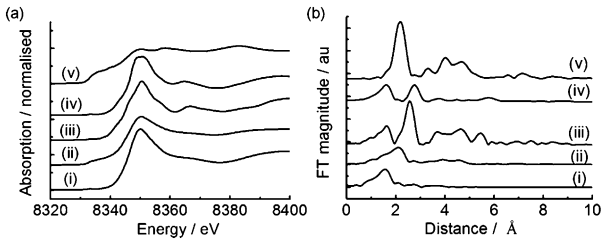

Figure 3. (a) XANES spectra and (b) Fourier-transformed EXAFS spectra collected from the Ni K-edge of (i) $TiNi_{pre}$, (ii) $TiNi_{cat}$, (iii) NiO, (iv) $Ni(OH)_2$, and (v) Ni foil.

ray absorption near-edge structure (XANES) of the Ni K-edge measured from FTO|$TiNi_{pre}$ and FTO|$TiNi_{cat}$. For comparison, the XANES of Ni foil, $Ni(OH)_2$ and NiO were also measured. The absorption edge position and high peak intensity in the $TiNi_{pre}$ XANES spectrum is consistent with the Ni species having a higher formal oxidation state than $TiNi_{cat}$ and similar electronic characteristics to $Ni(OH)_2$ and NiO. The Fourier-transformed Ni extended X-ray absorption fine structure (FT EXAFS) $\chi(k)k^2$ spectrum of hydrolyzed $TiNi_{pre}$ shows a peak around 1.6 Å, corresponding to the presence of O in the first coordination shell of the Ni (Figure 3b). In the case of $TiNi_{cat}$, the shape of the XANES spectrum is an intermediate between that of the Ni–O solids and metallic Ni. The Ni EXAFS $\chi(k)k^2$ spectrum of $TiNi_{cat}$ shows a peak of around 2 Å in the FT, with a small shoulder extending into the smaller reduced distances. This is consistent with the Ni having an average coordination environment more similar to that of Ni metal, with a small proportion of Ni–O species. Synergistic effects of NiO and Ni for HER under basic conditions have recently been demonstrated[10] and may also be responsible for the higher activity of $TiNi_{cat}$ compared to $TiNi_{pre}$ and e-Ni.

Both the XANES and EXAFS of the Ti K-edge reveal that the dominant Ti species before and after cathodic activation of TiNi closely resembles the oxidation state and coordination environment of TiO_2 (see the Supporting Information, Figure S9). This is consistent with the formation of TiO_2 after $TiNi_{pre}$ hydrolysis. Following cathodic activation, the Ti species within $TiNi_{cat}$ remains as TiO_2 trapped in an amorphous mixture containing the Ni–O and Ni metal species.

$TiNi_{cat}$ was subsequently investigated as a dual stabilizing and HER electrocatalyst layer on a planar p-Si substrate. Commercial p-Si wafers were employed as the light-absorbing semiconductor,[11] and $TiNi_{pre}$ was coated onto the p-Si electrode (p-Si|TiNi) by drop casting the TiNi solution (8×12.6 μL, 2.5 mM in toluene) on p-Si (0.42 cm^2 exposed surface area). The activation process for p-Si|TiNi involved holding p-Si|TiNi at 0 V vs. RHE under solar light irradiation in an aqueous B_i solution (0.1 M, pH 9.2) with KCl (1 M) as electrolyte (see the Supporting Information, Figures S10 and S11). A saturation photocurrent was reached after approximately 10 min.

Figure 4 compares the photoresponse of p-Si|$TiNi_{cat}$, bare p-Si, Ni-modified Si (p-Si|Ni), TiO_2-coated p-Si (p-Si|TiO_2), adjacent layers of TiO_2 and Ni on p-Si (p-Si|TiO_2|Ni), and Pt-modified Si (p-Si|Pt) photoelectrodes under chopped solar light irradiation (AM 1.5G). The Pt and Ni electrocatalysts were photodeposited onto p-Si electrodes by chronopotentiometry with a current density of 40 μA cm^{-2} for approximately 5 min under UV/Vis irradiation (see the Supporting Information). TiO_2 layers were coated onto the p-Si surface by the drop casting of titanium isopropoxide (8×12.6 μL, 2.5 mM in toluene). Pt serves as a reference benchmark catalyst for the $TiNi_{cat}$ HER catalyst.

The p-Si|$TiNi_{cat}$ photocathode exhibited excellent photoresponse with an onset potential for HER of approximately 0.3 V

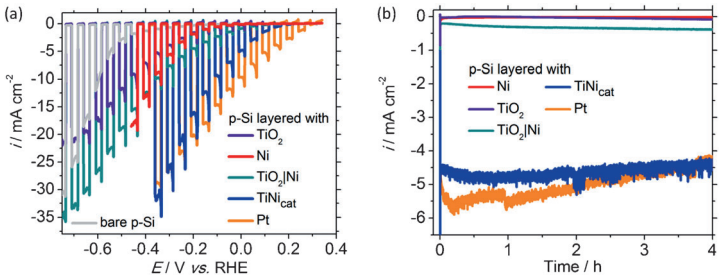

Figure 4. (a) LSV scans measured in an aqueous pH 9.2 electrolyte solution (0.1 M B_i and 1 M KCl) under chopped solar light irradiation (AM 1.5G) with a scan rate of 5 mV s^{-1}. (b) Chronoamperometry of photocathodes recorded at 0 V vs. RHE under solar light irradiation (AM 1.5G) for 4 h.

vs. RHE, which is close to the valence band potential in p-Si of approximately 0.5 V vs. RHE.[12] A photocurrent of −5 mA cm^{-2} was observed at 0 V vs. RHE, which is approximately 10-fold higher than that of p-Si coated with separate layers of TiO_2 and Ni. The p-Si|$TiNi_{cat}$ shows an incident photon-to-current conversion efficiency (IPCE) between 40 and 50% and an absorbed photon-to-current conversion efficiency (APCE) of 55–74% when irradiating with $\lambda = 400$ to 800 nm (0.2–0.6 mW cm^{-2}) at an applied potential of 0 V vs. RHE (see the Supporting Information, Figure S12). A bare p-Si electrode (without electrocatalyst), p-Si with electrodeposited Ni or a drop-casted TiO_2 layer exhibited comparably poor photoactivity, producing photocurrents of less than −0.4 mA cm^{-2} at 0 V vs. RHE (Figure 4).

The benchmark p-Si|Pt photocathode has a more positive onset potential than p-Si|$TiNi_{cat}$; a photocurrent onset potential of approximately 0.4 V with a current density of −9 mA cm^{-2} at 0 V vs. RHE was observed. Both p-Si|$TiNi_{cat}$ and p-Si|Pt exhibit an anodic shift in onset potential, which indicates reduced surface recombination due to a reduced kinetic/electron-transfer barrier at the photocathode surface, and the increased electrochemical activity on the p-Si substrate. A more positive onset potential may be achieved by using different strategies, for example, by using very thin insulating layers between $TiNi_{cat}$ and p-Si to electrically decouple those two layers.[12]

Photocathodes fabricated with $TiNi_{cat}$ also exhibit good stability with a negligible decrease in the photocurrent after 4 h of continuous solar light irradiation (Figure 4b and S13). The p-

 © 2015 The Authors. Published by Wiley-VCH Verlag GmbH & Co. KGaA, Weinheim

Si|$TiNi_{cat}$ electrode exhibited a half-life time of 12 h and displayed a comparable photostability to p-Si|Pt. We observed that the catalytic coatings flaked off from the vigorous H_2 bubbling and the long-term stability of both electrodes appears therefore to be compromised by physical instability. Without the protective layer of $TiNi_{cat}$ or Pt, the activity of bare p-Si significantly drops within a few minutes. To confirm that the photocurrent of p-Si|$TiNi_{cat}$ was due to HER, photoelectrolysis was performed at 0 V vs. RHE under solar light irradiation using headspace gas analysis by gas chromatography. After 1 h, 6.1 ± 0.8 C passed through the outer circuit and 31 ± 4 μmol of H_2 were detected with an exposed area of 0.42 cm^2, corresponding to quantitative faradaic efficiency (Table 1).

The limiting factor of the PEC activity in p-Si|$TiNi_{cat}$ can be understood by considering the (photo)electrochemical response of FTO|$TiNi_{cat}$, FTO|Pt and p-Si|Pt in Figure 5. The photocurrent measured at a photoelectrode is limited by the reaction kinetics at the electrode surface, the electron–hole separation efficiency in the bulk semiconductor substrate and/or light absorption. FTO|$TiNi_{cat}$ shows a current density of approximately -6 mA cm^{-2} at -0.6 V vs. RHE. This potential corresponds to the Si conduction band potential and the current of FTO|$TiNi_{cat}$ at -0.6 V vs. RHE is indeed close to the photocurrent of -5.0 mA cm^{-2} at 0 V vs. RHE generated by the p-Si|$TiNi_{cat}$ electrode under AM 1.5 light irradiation (100 mW cm^{-2}; Figures 2b and 5). This observation suggests that the performance of p-Si|$TiNi_{cat}$ is limited by the HER kinetics of $TiNi_{cat}$.

In contrast, a current density of approximately -19 mA cm^{-2} was generated by FTO|Pt at -0.6 V vs. RHE, which may correspond to the maximum current density obtainable with the conduction-band electrons of p-Si (Figure 5). However, a photocurrent of -9 mA cm^{-2} was produced by the p-Si|Pt electrode at 0 V vs. RHE. This suggests that the performance of this photocathode was limited by the photoactivity of p-Si and not the HER kinetics of the Pt. Consistently, the photocurrent of p-Si|Pt is dependent on the light intensity (see the Supporting Information, Figure S14). Hence, despite Pt being a more efficient electrocatalyst than $TiNi_{cat}$, the p-Si|Pt photocathode shows only a small improvement compared to p-Si|$TiNi_{cat}$ due to the intrinsic activity limitation of p-Si. Thus, $TiNi_{cat}$ shows good performance as a non-noble HER catalyst, operates under near-neutral conditions,[6,7] and it can even show an activity close to Pt when deposited on p-Si.

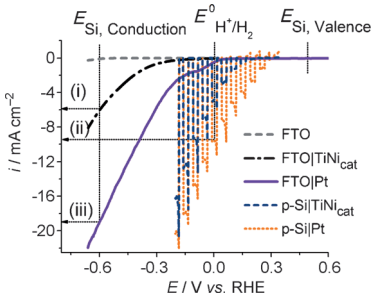

Figure 5. A comparison of the electrochemical profile of FTO|$TiNi_{cat}$ and FTO|Pt with the PEC profile of p-Si|$TiNi_{cat}$ and p-Si|Pt to understand the PEC mechanism and factors limiting performance. LSV scans of FTO|Pt, FTO|$TiNi_{cat}$, and FTO electrodes for electrocatalytic HER (dark reaction) at 1 mV s^{-1}, and of p-Si|Pt photocathode and p-Si|$TiNi_{cat}$ recorded under chopped solar light irradiation (AM 1.5G) at 5 mV s^{-1}. Experiments were conducted in an aqueous pH 9.2 solution (0.1 M B_i and 1 M KCl). (i) and (iii) indicate the electrocatalytic proton reduction current measured at FTO|$TiNi_{cat}$ and FTO|Pt, respectively, at the p-Si conduction band potential of -0.6 V vs. RHE; (ii) shows the photocurrent of p-Si|Pt recorded at 0 V vs. RHE under simulated solar light irradiation (AM 1.5G).

Other promising non-noble HER catalysts that have been fabricated on crystalline p-Si to form a hybrid photocathode include nickel–molybdenum (Ni–Mo),[5g] molybdenum disulfide (MoS_2),[5d,e] and tungsten carbide (W_2C).[5c] Compared to these previously reported Si electrodes, p-Si|$TiNi_{cat}$ exhibits a favorable anodic onset potential and comparable photostability and does not require acidic conditions. The high photoactivity of p-Si|$TiNi_{cat}$ under neutral–alkaline conditions is important, because most non-noble metal-based O_2 evolution electrocatalysts and photoanodes are only functional in neutral or alkaline conditions. However, operating close to pH neutral conditions can give rise to a pH gradient at the electrode surface.[13] This may lead to a non-optimal fill factor, which would limit the HER photocurrent in the underpotential region ($E > 0$ V vs. RHE). Regardless, research close to pH 7 is still essential for eco-friendly future technologies, where abundant water supplies such as river water and seawater are employed. p-Si|$TiNi_{cat}$ is therefore an attractive non-noble metal photocathode with good compatibility with photoanodes for overall solar water splitting. Furthermore, unlike the preparation procedures of the aforementioned hybrid photocathodes, the preparation of p-Si|$TiNi_{cat}$ is very simple and scalable, without requiring costly equipment and procedures.

In summary, we report a novel, non-noble hybrid photocathode that operates at high efficiency and with good photostability under near pH neutral conditions. This p-Si|$TiNi_{cat}$ photocathode is very easy to prepare and makes use of single-source precursor chemistry, which gives much scope to explore other molecular precursors to further improve the performance of the hybrid electrodes in the future.[14] The $TiNi_{cat}$ film is formed through a dual activation process—hydrolysis and in situ cathodic treatment. This novel composite phase consists of metallic Ni embedded in an amorphous NiO/$Ni(OH)_2$ and TiO_2 matrix and is difficult to access through conventional synthetic routes. This $TiNi_{cat}$ film forms an excellent interface with p-Si, simultaneously passivating the p-Si semiconductor and activating it for HER catalysis. The passivated p-Si|$TiNi_{cat}$ electrode displays a promising stability, which even allows it to be handled under ambient conditions. During operation, it generates photocurrents of approximately 5 mA cm^{-2} in an aqueous pH 9.2 solution at 0 V vs. RHE with a quantitative faradaic efficiency for several hours under 1 sun illumination. p-Si|$TiNi_{cat}$ therefore sets a novel benchmark for a H_2-evolving photocathode constructed solely from earth-abundant materials that operates efficiently under neutral–alkaline conditions.

Acknowledgements

Financial support from the Christian Doppler Research Association (Austrian Federal Ministry of Science, Research and Econo-

 © 2015 The Authors. Published by Wiley-VCH Verlag GmbH & Co. KGaA, Weinheim

my and National Foundation for Research, Technology and Development), the OMV Group and the EPSRC (EP/H00338X/2) is gratefully acknowledged. D.S.W. thanks the ERC for an Advanced Grant, Y.H.L. the Cambridge Trust and J.Z.Z. the European Commission for a Marie Curie IIF Fellowship (PIIF-GA-2012-328085 RPSII). We also thank the National EPSRC XPS User's Service (NEXUS) at Newcastle University, an EPSRC Mid-Range Facility for XPS measurements. The authors also appreciate Diamond Light Source for the allocation of beam time (SP11099) and support by their staff.

Keywords: hydrogen evolution · photocatalysis · photosynthesis · silicon · water splitting

[1] a) A. C. Nielander, M. R. Shaner, K. M. Papadantonakis, S. A. Francis, N. S. Lewis, *Energy Environ. Sci.* **2015**, *8*, 16 – 25; b) J. R. McKone, N. S. Lewis, H. B. Gray, *Chem. Mater.* **2014**, *26*, 407 – 414; c) T. J. Jacobsson, V. Fjällström, M. Edoff, T. Edvinsson, *Energy Environ. Sci.* **2014**, *7*, 2056 – 2070; d) T. Hisatomi, J. Kubota, K. Domen, *Chem. Soc. Rev.* **2014**, *43*, 7520 – 7535; e) S. Hu, M. R. Shaner, J. A. Beardslee, M. Lichterman, B. S. Brunschwig, N. S. Lewis, *Science* **2014**, *344*, 1005 – 1009; f) C.-Y. Lin, D. Mersch, D. Jefferson, E. Reisner, *Chem. Sci.* **2014**, *5*, 4906 – 4913; g) H. S. Park, C.-Y. Lee, E. Reisner, *Phys. Chem. Chem. Phys.* **2014**, *16*, 22462 – 22465; h) C.-Y. Lin, Y.-H. Lai, D. Mersch, E. Reisner, *Chem. Sci.* **2012**, *3*, 3482 – 3487.

[2] a) B. A. Pinaud, J. D. Benck, L. C. Seitz, A. J. Forman, Z. Chen, T. G. Deutsch, B. D. James, K. N. Baum, G. N. Baum, S. Ardo, H. Wang, E. Miller, T. F. Jaramillo, *Energy Environ. Sci.* **2013**, *6*, 1983 – 2002; b) M. C. Hanna, A. J. Nozik, *J. Appl. Phys.* **2006**, *100*, 074510; c) R. T. Ross, T.-L. Hsiao, *J. Appl. Phys.* **1977**, *48*, 4783 – 4785.

[3] B. A. Parkinson, J. Turner in *Photoelectrochemical Water Splitting: Materials, Processes and Architectures*, The Royal Society of Chemistry, **2013**, pp. 1 – 18.

[4] M. A. Green, K. Emery, Y. Hishikawa, W. Warta, E. D. Dunlop, *Progress in Photovoltaics: Research and Applications* **2014**, *22*, 701 – 710.

[5] a) B. Seger, T. Pedersen, A. B. Laursen, P. C. K. Vesborg, O. Hansen, I. Chorkendorff, *J. Am. Chem. Soc.* **2013**, *135*, 1057 – 1064; b) N. P. Dasgupta, C. Liu, S. Andrews, F. B. Prinz, P. Yang, *J. Am. Chem. Soc.* **2013**, *135*, 12932 – 12935; c) S. P. Berglund, H. He, W. D. Chemelewski, H. Celio, A. Dolocan, C. B. Mullins, *J. Am. Chem. Soc.* **2014**, *136*, 1535 – 1544; d) Q. Ding, F. Meng, C. R. English, M. Cabán-Acevedo, M. J. Shearer, D. Liang, A. S. Daniel, R. J. Hamers, S. Jin, *J. Am. Chem. Soc.* **2014**, *136*, 8504 – 8507; e) J. D. Benck, S. C. Lee, K. D. Fong, J. Kibsgaard, R. Sinclair, T. F. Jaramillo, *Adv. Energy. Mater.* **2014**, *4*, 1400739; f) Y. Hou, B. L. Abrams, P. C. K. Vesborg, M. E. Björketun, K. Herbst, L. Bech, A. M. Setti, C. D. Damsgaard, T. Pedersen, O. Hansen, J. Rossmeisl, S. Dahl, J. K. Norskøv, I. Chorkendorff, *Nat. Mater.* **2011**, *10*, 434 – 438; g) J. R. McKone, E. L. Warren, M. J. Bierman, S. W. Boettcher, B. S. Brunschwig, N. S. Lewis, H. B. Gray, *Energy Environ. Sci.* **2011**, *4*, 3573 – 3583.

[6] C. He, X. Wu, Z. He, *J. Phys. Chem. C* **2014**, *118*, 4578 – 4584.

[7] S. Cobo, J. Heidkamp, P.-A. Jacques, J. Fize, V. Fourmond, L. Guetaz, B. Jousselme, V. Ivanova, H. Dau, S. Palacin, M. Fontecave, V. Artero, *Nat. Mater.* **2012**, *11*, 802 – 807.

[8] Y.-H. Lai, T. C. King, D. S. Wright, E. Reisner, *Chem. Eur. J.* **2013**, *19*, 12943 – 12947.

[9] J. Yu, Y. Hai, B. Cheng, *J. Phys. Chem. C* **2011**, *115*, 4953 – 4958.

[10] M. Gong, W. Zhou, M.-C. Tsai, J. Zhou, M. Guan, M.-C. Lin, B. Zhang, Y. Hu, D.-Y. Wang, J. Yang, S. J. Pennycook, B.-J. Hwang, H. Dai, *Nat. Commun.* **2014**, *5*, 4695.

[11] a) H. D. Abruña, A. J. Bard, *J. Am. Chem. Soc.* **1981**, *103*, 6898 – 6901; b) S. W. Boettcher, J. M. Spurgeon, M. C. Putnam, E. L. Warren, D. B. Turner-Evans, M. D. Kelzenberg, J. R. Maiolo, H. A. Atwater, N. S. Lewis, *Science* **2010**, *327*, 185 – 187; c) B. Seger, A. B. Laursen, P. C. K. Vesborg, T. Pedersen, O. Hansen, S. Dahl, I. Chorkendorff, *Angew. Chem. Int. Ed.* **2012**, *51*, 9128 – 9131; *Angew. Chem.* **2012**, *124*, 9262 – 9265.

[12] D. V. Esposito, I. Levin, T. P. Moffat, A. A. Talin, *Nat. Mater.* **2013**, *12*, 562 – 568.

[13] J. Jin, K. Walczak, M. R. Singh, C. Karp, N. S. Lewis, C. Xiang, *Energy Environ. Sci.* **2014**, *7*, 3371 – 3380.

[14] Y.-H. Lai, C.-Y. Lin, Y. Lv, T. C. King, A. Steiner, N. M. Muresan, L. Gan, D. S. Wright, E. Reisner, *Chem. Commun.* **2013**, *49*, 4331 – 4333.

Received: December 19, 2014
Published online on February 4, 2015

 © 2015 The Authors. Published by Wiley-VCH Verlag GmbH & Co. KGaA, Weinheim